


Article

Optimal Energy Management of EVs at Workplaces and Residential Buildings Using Heuristic Graph-Search Algorithm

Md Jamal Ahmed Shohan ^{1,2,*} , Md Maidul Islam ^{1,3}, Sophia Owais ^{1,2} and Md Omar Faruque ^{1,2} 

¹ Department of Electrical and Computer Engineering, FAMU-FSU College of Engineering, Florida State University, Tallahassee, FL 32310, USA; mislam@epri.com (M.M.I.); sowais@fsu.edu (S.O.); mfaruque@eng.famu.fsu.edu (M.O.F.)

² Center for Advanced Power Systems (CAPS), Florida State University, Tallahassee, FL 32310, USA

³ Electric Power Research Institute (EPRI), Knoxville, TN 37932, USA

* Correspondence: ms19bi@fsu.edu

Abstract: As the adoption of electric vehicles (EVs) continues to rise, efficient scheduling methods that minimize operational costs are critical. This paper introduces a novel EV scheduling method utilizing a heuristic graph-search algorithm for cost minimization due to its admissible nature. The approach optimizes EV charging and discharging schedules by considering real-time energy prices and battery degradation costs. The method is tested on systems with solar generation, electric loads, and EVs featuring vehicle-to-grid (V2G) connections. Various charging rates, such as standard, fast, and supercharging, along with uncertainties in EV arrival and departure times, are factored into the analysis. Results from various case studies demonstrate that the proposed method outperforms popular heuristic optimization techniques, such as particle swarm optimization and genetic algorithms, by 3–5% for different real-time energy prices. Additionally, the method's effectiveness in reducing operational costs for workplace EVs is confirmed through extensive case studies under varying uncertain conditions. Finally, the system is implemented on a digital real-time simulator with DNP3 communication, where real-time results align closely with offline simulations, confirming the algorithm's efficacy for real-world applications.



Citation: Shohan, M.J.A.; Islam, M.M.; Owais, S.; Faruque, M.O. Optimal Energy Management of EVs at Workplaces and Residential Buildings Using Heuristic Graph-Search Algorithm. *Energies* **2024**, *17*, 5278. <https://doi.org/10.3390/en17215278>

Academic Editors: Islam Safak Bayram, Emil Cazacu, Marilena Stanculescu and Sorin Deleanu

Received: 30 August 2024

Revised: 4 October 2024

Accepted: 22 October 2024

Published: 23 October 2024



Copyright: © 2024 by the authors. Licensee MDPI, Basel, Switzerland. This article is an open access article distributed under the terms and conditions of the Creative Commons Attribution (CC BY) license (<https://creativecommons.org/licenses/by/4.0/>).

Keywords: electric vehicles; graph-search algorithm; charging-discharging scheduling; energy storage; digital real-time simulation

1. Introduction

Electric vehicles are gaining popularity over conventional fossil fuel-based vehicles due to their low carbon footprint, and government subsidies. Additionally, using electricity to fully charge an EV is less expensive than having a similar-sized vehicle's tank filled with gasoline. Large-scale integration of EV charging stations makes the power grid susceptible to voltage fluctuation, frequency excursion, peak demand, etc. [1]. In order to combat this issue, real-time pricing strategies are increasingly being used by utility companies to shift peak demand to off-peak hours [2]. This feature can be used for optimal EV scheduling by determining the ideal time to charge EVs [3]. EVs can also be used as energy storage to sell energy to the grid with a vehicle-to-grid (V2G) connection [4]. Ideally, EVs should charge during low-price periods and discharge during peak-price periods. However, EVs are expected to be charged fully or partially before they are on the road. So, some constraints need to be addressed when solving EV scheduling problems. In addition, the uncertain nature of users' commuting behavior, price of electricity, traffic conditions, arrival and departure time of EVs, etc., make it difficult to find the optimal solution to this problem with a normal approach.

Researchers have suggested various strategies to find the best answer to this scheduling issue for EV charging and discharging [5–8]. For instance, the authors of [9] formulated a rule-based energy management mechanism to control the flow of energy of the EV where

they considered 10 different scenarios. The authors of [10] presented a comprehensive review of the scheduling of EVs where different methodologies used for this application were discussed. The authors of [11] proposed a two-stage framework for the economic operation of EV parking decks that took the uncertainty of rooftop photovoltaic panels into account. The authors of [12] proposed a two-level EV charging management system with stochastic programming while considering the integration of DERs for workplace EV charging stations. In both articles, users are unable to control the target state of charge (SoC) of EVs, which could be problematic if the EVs have to travel a significant distance. A stochastic energy management solution was proposed in [13] for EVs at parking lots equipped with distributed energy resources (DERs) while considering the unpredictable nature of energy price, and arrival and departure schedule of EVs. The authors of [14] proposed a multilayer iterative stochastic dynamic programming framework for energy management in smart buildings with integrated EVs, effectively adapting to fluctuating demand and dynamic energy prices, which is crucial for real-world applications.

In [15], a novel iterated random operator theory was developed to schedule the charging periods of EVs at charging stations with various charge levels. However, the authors failed to consider the degradation cost of the EV battery in the scheduling problem. The authors of [16] proposed an ordinal-based approach to find the optimum solution for real-time EV charging scheduling. The objective of the papers was to find a less computationally expensive method for the scheduling as the algorithm would be functioning in real time. The authors of [17] used a novel distributed simulation-based policy improvement method to coordinate multiple charging stations in a micro-grid environment while considering wind power generations. Recently, machine learning-based approaches such as reinforcement learning [18] and deep reinforcement learning [19] have been used by researchers to solve the scheduling problem of EV charging. The authors of [20] suggested a safe deep reinforcement learning method to reduce the cost of charging EVs using a constrained Markov decision process while still ensuring that they can be fully charged. However, most of the articles only considered one charging mode in their test cases. As various versions of charging modes are being used in real charging stations, the impacts of fast or supercharging for EV charging scheduling problems need to be discussed.

In order to schedule EV charging and discharging economically at the household level and workplace level with the integration of photovoltaic (PV) generation, this paper suggests a heuristic graph-search-based algorithm to minimize the cost of vehicle operation. This algorithm has recently been used to resolve the power system's optimization problems [21–23]. The proposed heuristic graph-search algorithm directly finds the optimal path by evaluating the actual and heuristic costs of each possible solution node unlike PSO and GA, which rely on population-based iterations to approximate solutions. This enables the algorithm to navigate the solution space more effectively by considering both current and future costs. This approach ensures that it always converges to the optimal solution without requiring multiple population updates or fitness evaluations, which can slow down PSO and GA. The graph-search algorithm excels in handling complex, non-linear constraints, such as battery degradation, real-time electricity prices, and uncertain EV departure/arrival times, something traditional meta-heuristics can struggle with due to their stochastic nature. This results in more precise and reliable scheduling outcomes under uncertainty. Machine learning (ML) models such as deep learning function as a black box, whereas the graph-search algorithm provides clear, explainable optimization paths for EV scheduling, which is crucial in energy management applications. Additionally, the proposed algorithm is computationally efficient and suitable for real-time applications, allowing timely decisions without the need for extensive computational resources or large datasets, which ML models typically require. The proposed method is also more adaptable to uncertainties in real-time data and scalable across different scenarios without requiring retraining. Although ML models can be powerful for complex prediction tasks, they are less practical in dynamic optimization settings like EV scheduling, where real-time adjustments and data variability are common.

This paper considers three charging modes for residential EV charging: (i) onboard normal charging, (ii) fast charging, and (iii) supercharging. It is common to have fast or rapid charging points at the workplace along with the onboard or standard charging points due to their direct access to a three-phase power supply [24]. The charging stations at the workplace generally have normal and level 2 fast charging capabilities [25]. So, this paper considers these two charging modes for the workplace level: (i) onboard normal charging, and (ii) fast charging. The main contributions of the paper are summarized below:

- The paper proposes a novel heuristic graph-search-based algorithm for the optimal management of EV charging and discharging at workplaces and residential buildings. The algorithm is compared with two traditional meta-heuristic methods to validate its effectiveness for this problem.
- The algorithm optimizes based on 24 h ahead electricity prices and vehicle-specific battery degradation costs. It also accounts for the inherent uncertainties in EV departure and arrival times and their SoC levels
- Two different real-time prices (RTPs) of electricity were used to test the robustness of the system, and these cases were designed to observe various battery operation strategies, including controlled charging, smart charging/discharging, and uncontrolled charging modes.
- A real-time testbed, employing the Distributed Network Protocol (DNP3)—a standard in electric power system communications—was modeled on real-time simulators to validate the proposed algorithm.

The remainder of this paper is structured as follows. The mathematical formulation of the problem is covered in Section 2. The mathematical representation and the flow chart of the suggested algorithm are provided in Section 3. Section 4 includes cost analyses based on offline simulation results, test cases, and system parameters. Real-time validation of the algorithm is provided in Section 5. Finally, Section 6 ends with concluding statements.

2. Problem Formulation

The proposed EV controller will have the objective of minimizing the cost of EV operation at residences and workplaces without violating any constraints. The algorithm's output will send control signals for the battery operation, such as charging or discharging the car, while it is connected to the power source. An accurate model for the battery is necessary to express its voltage, current, and SoC. The battery of EVs is modeled based on a Li-ion battery whose discharge curve can be segmented into three zones [26–28], as shown in Figure 1. The initial zone (Zone 1) reflects the exponential drop in the voltage of the cell during the initial discharge. The next segment (Zone 2) signifies the amount of charge extractable from the cell before reaching its nominal voltage. The final section (Zone 3) represents the complete discharge of the cell and its cutoff voltage. The model's parameters are deduced from the discharge characteristics and assumed to be the same for charging. Furthermore, it is assumed that the internal resistance of the cell remains constant during both charging and discharging cycles.

Equations (1) and (2) represent the charging and discharging equations, respectively [29].

$$V_{b,ev} = E_0 - Ri - K \frac{Q}{it - 0.1Q} \cdot i^* - K \frac{Q}{Q - it} \cdot it + Ae^{-B \cdot it} \quad (1)$$

$$V_{b,ev} = E_0 - Ri - K \frac{Q}{Q - it} \cdot i^* - K \frac{Q}{Q - it} \cdot it + Ae^{-B \cdot it} \quad (2)$$

where $V_{b,ev}$ is the battery voltage of the EV, A is the exponential voltage, K is the polarization constant, E_0 is constant voltage, B is the exponential zone time constant inverse, Q is the charge capacity, i is the battery current, i^* is the filtered current, t is time, and R is internal resistance. During the fully charged voltage, the filtered current, i^* , and the extracted

charge, it , both become zero as the current step has just begun. So, the voltage of the battery when it is fully charged, V_{full} , can be represented by (3) [29].

$$V_{full} = E_0 - Ri + A \quad (3)$$

To calculate the voltage of the exponential area, B is approximated to be $\frac{3}{Q_{exp}}$ as the energy of the exponential term becomes closer to zero and i^* is equal to i during the steady state. So, the voltage of the exponential zone, V_{exp} , can be defined by (4) [29].

$$V_{exp} = E_0 - Ri - K \frac{Q}{Q - Q_{exp}} \cdot (Q_{exp} + i^*) + Ae^{\frac{-3}{Q_{exp}} \cdot Q_{exp}} \quad (4)$$

Similarly, the voltage of the nominal area V_{nom} is defined by (5) [29].

$$V_{nom} = E_0 - Ri - K \frac{Q}{Q - Q_{nom}} \cdot (Q_{nom} + i^*) + Ae^{\frac{-3}{Q_{nom}} \cdot Q_{nom}} \quad (5)$$

The thermal part of the battery modeling is implemented based on [30]. The reference signal used for charging and discharging is $\in \{0, 1\}$. The controller will reduce the costs and consequently save money for users with a V2G connection considering the RTP of energy. An objective function for a residential place is formulated to solve this cost minimization problem, which can be represented by (6).

$$\min \left\{ \sum_{t \in T} \left[r_{rtp,t} \Delta t \sum_{v \in V} (P_{v,t}^c - P_{v,t}^i) + \sum_{v \in V} C_v^d P_{v,t}^d \right] \right\} \quad (6)$$

where, $r_{rtp,t}$ is the real-time energy price at time t , $P_{v,t}^c$ and $P_{v,t}^i$ represent consumed power from the grid and injected power to the grid for every EV v at time t , and Δt is the time interval, and C_v^d is the degradation cost of the battery. Degradation cost is a critical parameter for EV battery scheduling due to the nature of V2G operation. The degradation cost is integrated directly into the optimization objective as a key cost component. When the algorithm makes decisions about when to charge or discharge an EV, it not only considers the real-time energy price but also the associated battery degradation cost. The objective function includes both the cost of charging/discharging based on the real-time price of electricity and the degradation cost, ensuring that the optimization balances the operational cost with the long-term impact on the battery's lifespan. In this formulation, the degradation cost influences the decision on when and how much to charge/discharge the battery. Charging at times with lower real-time prices might seem optimal initially, but when accounting for degradation cost, the algorithm prioritizes strategies that minimize unnecessary battery wear, extending the battery's life and reducing long-term costs. The battery degradation model used in this study is based on well-established principles that take into account the Depth of Discharge (DoD), the number of cycles, and the efficiency of the battery [31]. Degradation is quantified by considering the relationship between the battery's use and its overall lifespan, which is represented by (7), where C_v^d is the battery degradation cost of the vehicle v , C_v^{bat} is the cost of a new battery of the vehicle v , DoD is the desired depth of charge of the EV battery, n_{cyc} is the number of cycles guaranteed under DoD, E_v^{max} is the maximum capacity of the battery (kWh), and η_b is the overall efficiency of the battery.

$$C_v^d(DoD, n_{cyc}) = \frac{C_v^{bat}}{n_{cyc} \times E_v^{max} \times DoD \times \eta_b} (\$/kWh) \quad (7)$$

The objective function is subjected to specific equality and inequality constraints. Inequality constraints of the problem are provided by (8)–(10). SoC at any time t has to be limited by the maximum and minimum SoC levels of the battery. Similarly, consumed or injected power by the EV battery at each time t has to be bounded by the minimum and maximum power rating. The power balance constraint is provided by (11), where the

power coming from the grid has to be equal to the total consumed power by loads and EVs. $P_G(t)$ is grid power, $P_{pv}(t)$ is the output power of PV, and $\sum_{l \in L} P_l(t)$ is the total consumed power for all loads L at time t in (11). Equation (12) indicates that the SoC level at the end of the charging period should be equal to the desired SoC level set by the user. As the vehicle battery cannot be charged and discharged at the same time, constraints presented by (13) and (14) are used to ensure the battery operates in one mode, i.e., charging or discharging where $\delta_{v,t}^c, \delta_{v,t}^i, \alpha_{v,t}$ are constant terms $\in \{0, 1\}$.

$$SoC_v^{min} \leq SoC_{v,t} \leq SoC_v^{max} \quad (8)$$

$$P_v^{min} \leq P_{v,t}^c \leq P_v^{max} \quad (9)$$

$$P_v^{min} \leq P_{v,t}^i \leq P_v^{max} \quad (10)$$

$$P_G(t) = \sum_{l \in L} P_l(t) - P_{pv}(t) + \sum_{v \in V} (P_v^c(t) - P_v^i(t)) \quad (11)$$

$$SoC_v^{(t=end)} = SoC_v^{desired} \quad (12)$$

$$\frac{\delta_{v,t}^c P_{v,t}^c + \delta_{v,t}^i P_{v,t}^i}{P_{v,t}^c + P_{v,t}^i} = \alpha_{v,t}, \text{ where } P_{v,t}^c + P_{v,t}^i \neq 0 \quad (13)$$

$$\delta_{v,t}^c + \delta_{v,t}^i = \alpha_{v,t} \quad (14)$$

The SoC of EVs is calculated using (15), where $SoC_{v,t}$ is the state of charge of the vehicle v at time step t , $P_{v,t}^r$ is the rated power of the EV battery, and η_v^c , and η_v^d are the battery's efficiency terms for charging and discharging, respectively.

$$\Delta SoC_{v,t} = \begin{cases} \eta_v^c \frac{P_{v,t}^r \times \Delta t}{E_v^{max}}, & \text{when charging} \\ \frac{1}{\eta_v^d} \frac{P_{v,t}^r \times \Delta t}{E_v^{max}}, & \text{when discharging} \end{cases} \quad (15)$$

The problem formulation for a workplace with charging stations is the same as the residential level except for the objective function. The objective function considers another cost component called demand charge, C_{dc} , contributed by violating the peak demands while charging EVs. So, the objective function for a workplace with charging stations can be expressed by (16).

$$\min \left\{ \sum_{t \in T} \left[r_{rtp,t} \Delta t \sum_{v \in V} (P_{v,t}^c - P_{v,t}^i) + \sum_{v \in V} C_v^d P_{v,t}^d \right] + C_{dc} \max_{t \in T_m} (P_{v,t}^c) \right\} \quad (16)$$

Let us consider a distribution grid with a transformer, dynamic load, PV generation, EV, and power electronics, such as a DC-AC and a DC-DC converter, which are all part of a residential system. Figure 2 depicts the test systems' architecture. The PV and grid supply the majority of the dynamic loads at the household level. If additional PV generation occurs, the energy can be sold back to the grid. The EV's battery can be used as energy storage to power the load. The EV charging station also supports bi-directional power flow, which means the battery can inject power into the grid. Figure 2b shows the test system for a workplace with charging stations which consists of PV panels, EV charging panels, and power electronics components. EVs in the charging station also have the capability to discharge, i.e., inject power into the grid. The MATLAB/Simulink v2022a platform was used to model the test systems.

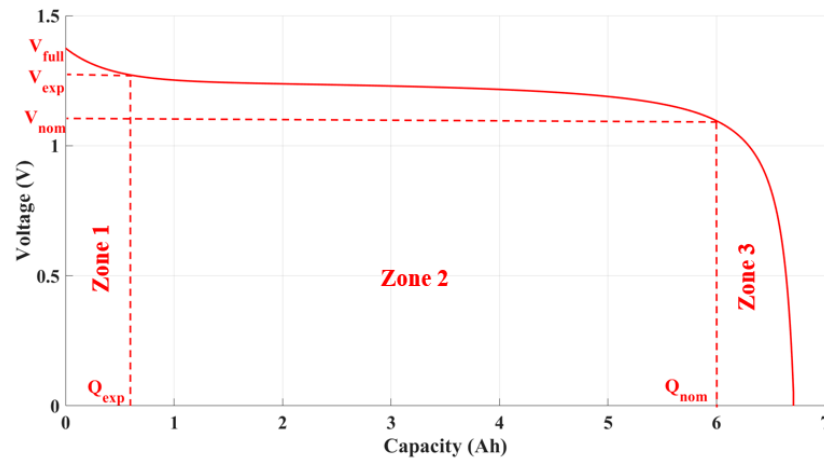


Figure 1. Discharge curve of a Li-ion battery [26–28].

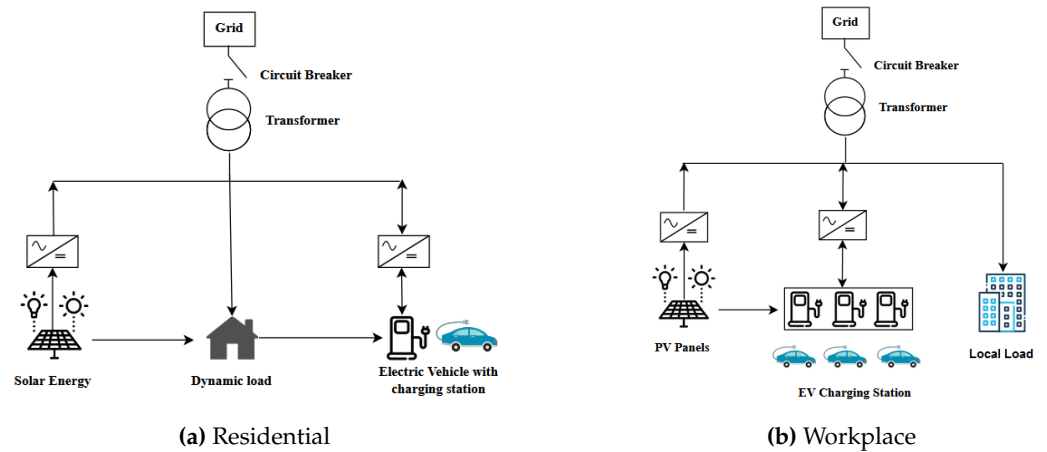


Figure 2. Architecture of test system models.

3. Proposed Algorithm

A heuristic graph-search-based algorithm known as A star (A^*) has been known for its use in robot path planning [32]. The main objective of a path planning problem is to navigate through terrain with numerous obstacles while finding the target location in the shortest amount of time possible. This issue is resolved by the A^* algorithm, which builds a graph of the terrain with numerous nodes and determines the path with the lowest cost. We can consider the target location as the target SoC level, and the nodes as the time steps necessary for each control action, making the EV scheduling problem a similar type of problem. Then, evaluating each path's cost after considering all the potential nodes, the best path can be found. The cost is calculated using (17), where n stands for the specific node.

$$f(n) = g(n) + h(n) \quad (17)$$

The total cost function, which is a combination of two other costs, is represented by the symbol $f(n)$ in this equation. One is the actual cost, or $g(n)$, which is the price incurred along the route taken to reach the node from the starting node. Heuristic cost, or $h(n)$, is the other cost and it calculates the price to travel to the target node from the node, n . The heuristic cost function must be accepted for the algorithm to always choose the cheapest route. It implies that the estimated heuristic cost cannot be greater than the actual path cost between the current node and the target node. As a result, the heuristic cost must be carefully calculated, which is problem-specific. A^* begins by figuring out the total cost of all the nodes that are closest to the starting node. All of these closest nodes, which are also referred to as the initial node's children, are added to a list called OPEN. Then, it selects the

node whose successor has the smallest cost function, $f(n)$. The starting node can now be referred to as the successor node's parent node. To determine its successor, the next step is to compute the total cost of the closed nodes of the predecessor node. The initial successor node is moved to a new list that is CLOSED after being removed from the OPEN list. After the next line of successor nodes has been added to the OPEN list, the node with the lowest cost is then selected as the succeeding successor. Until the heuristic cost is zero, or when it reaches the target node, the algorithm extends the OPEN and CLOSED lists. The CLOSED list contains all the nodes from the start to the goal node that have the lowest costs. To find the best path, the algorithm now retraces its steps from the starting node to the target node. Figure 3 contains the flow chart for the A* algorithm.

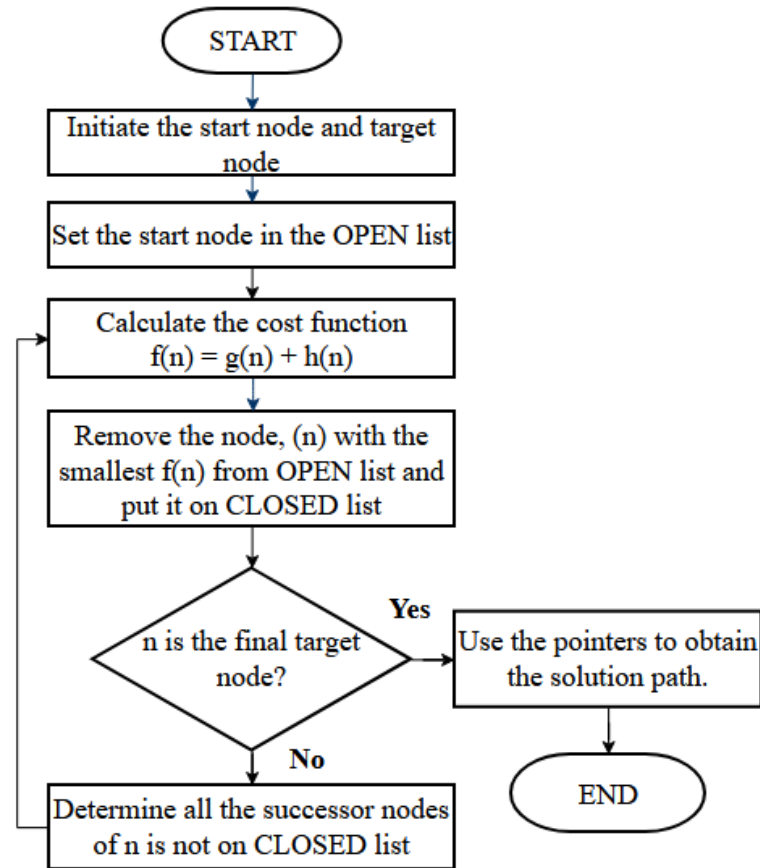


Figure 3. Flow chart of A* algorithm.

In order to implement this method for our case, at first, the solution space needs to be defined by a combination of nodes and edges. The starting node will be initiated using the current status of the system. The algorithm will have access to 24 h predicted RTP and load data to use for determining the future nodes and edges. The total actual cost from time t to time $t + \Delta T$ for the problem is represented by $C_{actual}(n)$. It can be calculated using (18), where $C_{EV}(pc)$ is the cost to go from parent node p to child node c , and $C_{lowest}(p)$ is the lowest cost to get to the parent node p from the starting node.

$$C_{actual}(n) = C_{EV}(pc) + C_{lowest}(p) \quad (18)$$

$C_{EV}(pc)$ is calculated using (19), where SoC_c and SoC_p represent the state of charge at the child and parent node, r_{rtp} is the real-time price of electricity from time t to time $t + \Delta T$, and ΔT is the time interval.

$$C_{EV}(pc) = (SoC_c - SoC_p) \cdot E_v^{max} \cdot r_{rtp} \quad (19)$$

The heuristic cost $C_h(n)$ of node n at time t can be calculated by (20), where $D(n)$ and $r_{rtp}(n)$ are the energy demand and real-time electricity price between time t and $t + \Delta T$, respectively.

$$C_h(n) = \sum_{n=t}^{\text{end}} D(n) \cdot r_{rtp}(n) \quad (20)$$

so, the total cost $C_{total}(n)$ can now be written as (21) for this problem.

$$C_{total}(n) = C_{actual}(n) + C_h(n) \quad (21)$$

Figure 4 provides a graphical representation of the solution space of EV SoC with the proposed algorithm. In the figure, the x-axis represents time $t = 0, \Delta T, 2 \times \Delta T, \dots, T$ where $\Delta T = 15$ min, T is the end time, and the y-axis represents SoC. Let us assume that at time $t = 0$, the initial SoC of the EV battery is 50%, and at time $t = T$, the desired SoC is 90%. The SoC of the EV battery is discretized in steps of 4% for the normal charging mode of Tesla Model 3. It is assumed that the battery can discharge a maximum of 8% at a time safely. Now, in the next time step, $t = \Delta T$, the battery's possible SoC can be 42%, 46%, 50%, or 54%. Similarly, all the nodes are formulated for the solution space until t reaches T . The cost to go from one node at $t = 0$ to another possible node at $t = \Delta T$ is calculated using (18), and the cost to go from the node $t = \Delta T$ to the final node at $t = T$ is calculated with (20). Based on all the costs, the algorithm will decide which path to take to obtain a cost-effective solution without violating constraints.

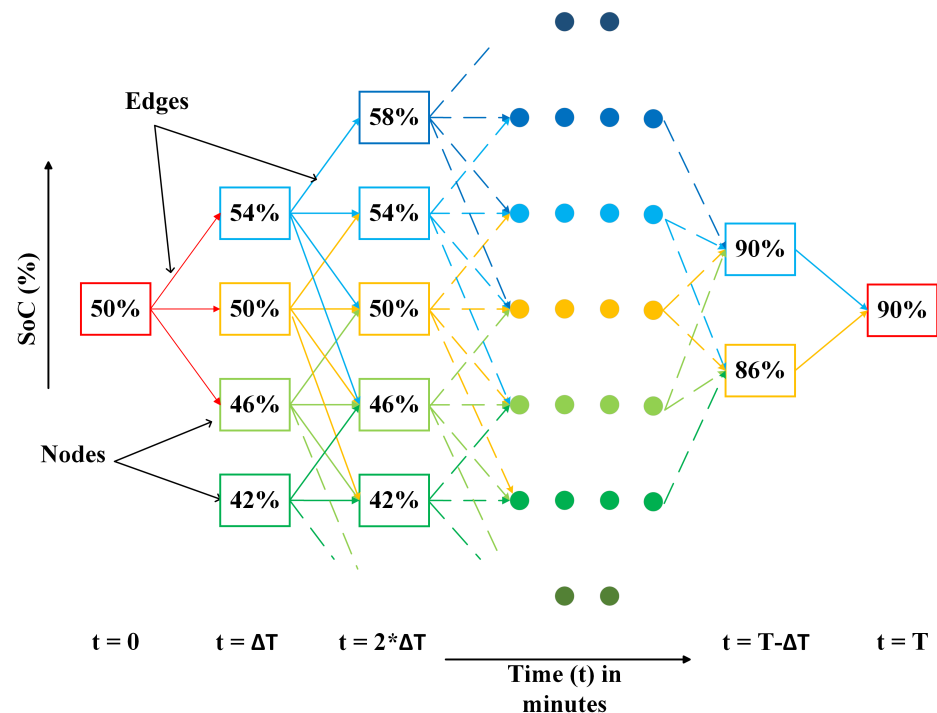


Figure 4. Demonstration of the discretized solution space of EV SoC with the A* algorithm.

The proposed algorithm will provide reference signals for charging and discharging for a time interval of 15 min. Users can set the algorithm's end time, i.e., the operation time of the vehicle and the desired SoC level of the vehicle. It is therefore possible for the controller to charge the EV to its maximum level before the start of the journey if any user plans to travel a long distance. The algorithm is based on 24 h ahead price forecasts, which provide a reasonable approximation of future energy costs. However, in dynamic energy markets, real-time prices may fluctuate due to demand response, market conditions, or renewable energy integration, potentially affecting the optimality of the

charging/discharging decisions. In this model, it is assumed that EVs will maintain their battery temperature at its optimal level, reducing the effects of temperature on the performance. The charging rate is linearized between the time steps to reduce model computational time based on the current SoC. The SoC of the battery will be sent from the vehicle itself, and using a charging profile, we almost accurately predict what its state of charge is going to be for the next time step. The flow of data required by the controller for its optimal EV charging and discharging schedule is depicted in Figure 5. Forecasted parameters can be obtained using machine learning methods, e.g., neural prophet [33], deep neural network [34], LSTM [35], etc. Historical datasets of the required parameters can be obtained from different independent system operators (ISOs). The controller will provide the reference signal for each EV based on all the data available to it.

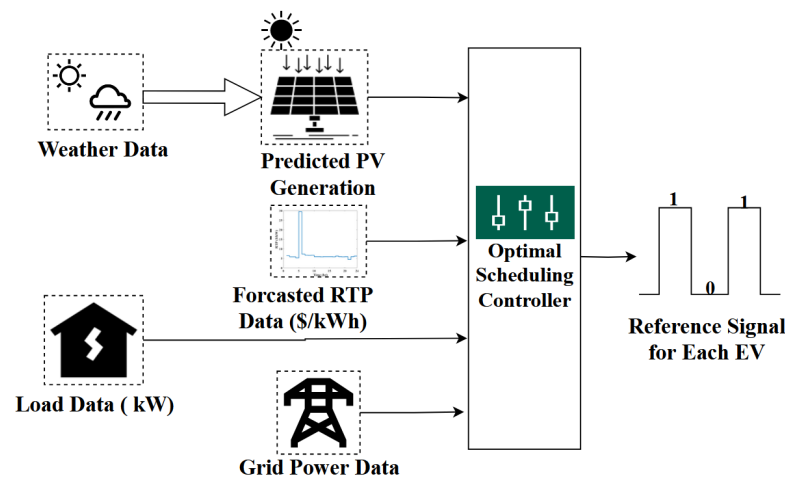


Figure 5. Data flow of EV scheduling controller.

All offline simulations were performed on a personal computer with Intel(R) Core(TM) i7-10510 CPU @ 1.8 GHz (Intel, Santa Clara, CA, USA) with 16 GB of RAM running on a 64-bit Windows 10 operating system.

4. Offline Results and Analysis

4.1. Residential

Due to the Tesla Model 3's variety of charging options, this vehicle was chosen as the EV model to test the proposed algorithm for residential purposes. The EV model parameters can be found in [36,37]. The Tesla Model 3 has a 240 V adapter for onboard standard charging. To charge the vehicle, a fast charger with a maximum power rating of 120 kW to 150 kW can be used. Tesla's supercharger version 3, with a maximum power rating of 250 kW, provides the fastest charging speed. The data for the test system, including solar generation and dynamic load profiles, are taken from [38]. All of the parameters used for the test system are listed in Table 1.

Table 1. EV battery test system parameters.

Parameter	Value	Parameter	Value
Battery Capacity	57.5 kW	SoC_{min}	10%
Max. Power for Normal Charging	11.5 kW	SoC_{max}	90%
Max. Power for Fast Charging	150 kW	DoD	80%
Max. Power for Supercharging	250 kW	n_{cyc}	380
Efficiency, η_v	90%	C_v^d	0.85 USD/kWh

Two RTP profiles were used to evaluate the controller's performance for the various test cases mentioned above. One energy price was obtained by modifying the New England

Independent System Operator (NEISO) [39] hourly locational marginal price (LMP) to match the daily average price of the Massachusetts region. Another synthesized price was created by combining the NYISO's marginal price [40] with the time-of-use (ToU) price of electricity in Tallahassee, Florida. This energy price was calculated in 15-min increments. Equations (22) and (23) are used to modify the NYISO price, where NY_{avg} is the average price of NYISO price, T_{off} is the off-peak bias, T_{on} is on-peak bias, S_c is supplier charge, $rt p_t^{off}$ is off-peak RTP at time t , and $rt p_t^{on}$ is on-peak RTP at time t . This synthesized price will be more appropriate to the North Florida market while preserving the fluctuating nature of RTP.

$$rt p_t^{off} = LMP_t + |NY_{avg} - T_{off}| + S_c \quad (22)$$

$$rt p_t^{on} = LMP_t + |NY_{avg} - T_{on}| + S_c \quad (23)$$

The following three test cases have been considered in order to test the controller algorithm.

4.1.1. Case I

In this case, the EV will start charging at 10:00 p.m. to reach its maximum level without the use of a controller. As a result, there will be no V2G operation in this case. This will serve as the baseline against which all other cases will be compared for cost analysis.

The average net cost of this operation for the user is –USD 3.50 for the NEISO-based energy price and –USD 1.95 for the synthesized Tallahassee energy price, respectively. In this case, a negative net cost means that users must pay that amount to the utility.

4.1.2. Case II

During the weekdays, people with families tend to leave early for work and return home in the afternoon [41]. In this case, 12 h (from 6:00 p.m. to 6:00 a.m.) was chosen for the EV's charging and discharging period, and the SoC level of the EV's battery had to be at its maximum (90%) at the end of the period. The initial SoC is set randomly between 40 and 80%.

EV profiles for both normal charging and supercharging modes are shown in Figure 6.

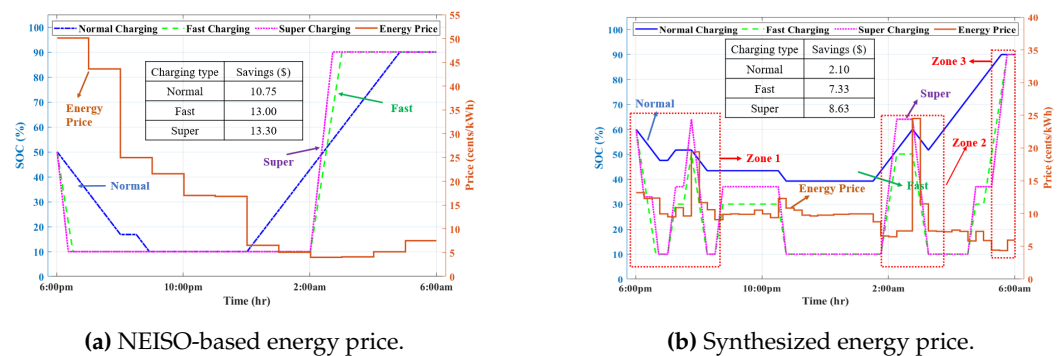


Figure 6. EV battery charging and discharging profile for 12 h operation.

The optimal scheduling of EV for NEISO-based energy price where energy price is high during the evening time is depicted in Figure 6a. As a result, the EV initially injects power into the grid before consuming power to charge to its set point before 6:00 AM (set by the user). Because the EV can be charged and discharged quickly with fast and supercharging, Figure 6a shows that only one charging and one discharging action are required to maximize the gain. As shown in Figure 6b, the proposed algorithm can maximize savings by discharging during peak prices based on predicted energy prices. For example, the EV discharged energy for all modes in Zone 1 and the SoC reached different levels based on its charging mode. In Zone 2, it can be seen the battery was charging at a lower price so that it could discharge during the peak price. The algorithm ensures that all

the actions taken by the battery lead up to its desired SoC level, which is represented in Zone 3 of Figure 6b. Overall savings for a day are calculated by (24), where $NC_{c,i}$ is the net cost with the proposed method, i represents different charging modes, and NC_{base} is the net cost when no control action was taken.

$$Savings_i = NC_{c,i} - NC_{base} \quad (24)$$

The savings using NEISO-based energy price are USD 10.75, USD 13.00, and USD 13.30 with normal charging, fast charging, and supercharging, respectively. Similarly, using the synthesized energy price, the net costs of normal, fast, and supercharging are USD 2.10, USD 7.33, and USD 8.63, respectively.

4.1.3. Case III

The assumption, in this case, is that the vehicle is available for 24 h (from 6:00 a.m. to 6:00 a.m. the following day) and must be fully charged at the end of that time. This type of scenario is common on the weekends.

The charging/discharging profiles for Case III are shown in Figure 7. In this case, the vehicle is available for charging and discharging for 24 h. The SoC of the EV drops to its lowest level during peak prices to maximize savings by discharging energy. The algorithm ensures that the EV battery has enough stored energy for maximum capitalization of the peak prices. The SoC then rises to its desired value during low-price periods. In this case, overall savings in 24 h for NEISO-based prices are USD 13.30, USD 21.60, and USD 21.60 for normal, fast, and supercharging modes. Charging and discharging during small fluctuations in energy price will damage the battery and as a result, the net cost will be higher. The algorithm ensures this by considering degradation cost and depth of charge, which are reflected in Figure 7b. The synthesized price fluctuated during the morning with small differences, so the battery was not charged. However, the price variation was high enough during the afternoon to charge/discharge the battery. In this case, overall savings in 24 h for synthesized-based prices are USD 4.53, USD 14.29, and USD 15.37 for normal, fast, and supercharging modes, respectively.

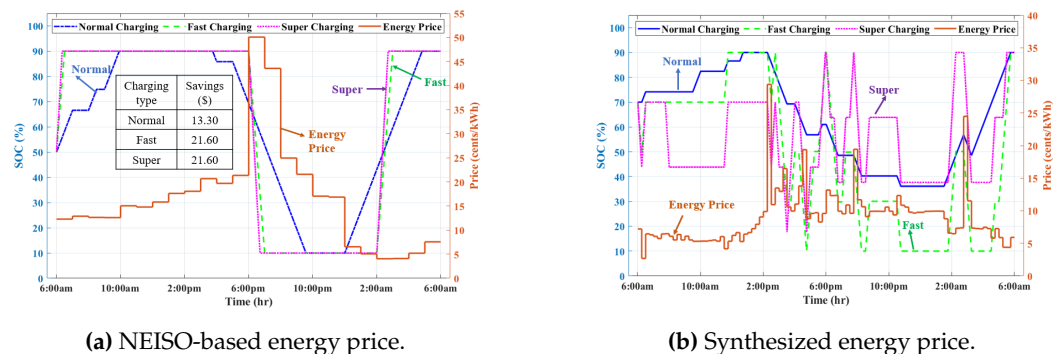


Figure 7. EV battery charging and discharging profile for 24-hour operation.

4.1.4. Comparison Analysis

The algorithm was compared with two meta-heuristic methods, i.e., particle swarm optimization (PSO) and genetic algorithm (GA), to show its efficacy over any meta-heuristic approach. PSO is a swarm-based optimization algorithm that is inspired by social animals' collective behavior [42]. Researchers have used this method for optimal dispatch problems [43] and scheduling problems for EV charging and discharging [44]. GA is a computational method inspired by biological evolution [45]. The main idea in GA is to find the best chromosomes from a random population of chromosomes based on the solution they provide. The authors of [46] used GA for smart charging and discharging schedules for EV fleets. These two methods were modeled using Python and the hyperparameters were optimized using the random search method. The selected population size and number of epochs were 100 and 400 for GA, and 120 and 200 for PSO, respectively. The algorithms

were simulated multiple times with different hyperparameters and specifying random seeds in order to find the optimal solution.

Table 2 provides the comparison analysis for the residential EV charging/discharging schedule with different techniques.

Table 2. Comparison analysis for different techniques.

Case No.	Charging Type	Savings (USD) for NEISO Based Price			Savings (USD) for Synthesized Based Price		
		A*	PSO	GA	A*	PSO	GA
Case II	Normal	10.75	10.25	10.40	2.10	1.98	2.03
	Fast	13.00	13.00	13.00	7.33	7.33	7.27
	Super	13.30	13.30	13.30	8.63	8.63	8.63
Case III	Normal	13.30	12.75	12.90	4.53	4.25	4.33
	Fast	21.60	21.60	21.60	14.29	14.29	14.29
	Super	21.60	21.60	21.60	15.37	15.37	15.37

Case I was used as a base case to calculate cost savings, as it represents normal operation without any controller action. Table 2 shows that A* always performs better in normal charging mode than other methods. However, almost all the methods perform similarly for fast and supercharging modes. In Case II, A* achieves 4.6% greater savings than GA and 3.2% greater savings than PSO in normal charging mode with NEISO-based pricing. For synthesized pricing, A* shows a 5.7% improvement over GA and a 3.33% improvement over PSO. In Case III, A* provides 5.6% better savings than GA and 4.% better than PSO in normal charging mode with NEISO-based pricing. For synthesized pricing, the improvements in savings with A* are 6.18% over GA and 4.44% over PSO. From the results, it can also be concluded that the supercharging option saves more money than the normal charging mode due to its high charging rate. However, the high installation costs of fast or supercharging facilities must be considered, as these may result in a longer return on investment period compared to the normal onboard charging operation. Table 3 provides the computational time for each method, where it can be observed that the proposed algorithm provides a faster solution than the other two methods.

Table 3. Computational time comparison.

Algorithm	Computational Time (s)
A*	124
PSO	145
GA	173

4.2. Workplace Building with EV Charging Station

For a quantitative evaluation, modeling a workplace equipped with an EV charging station is crucial for the decision-making process of optimal scheduling [47]. Additionally, it is important to determine the optimal strategy for different vehicles at charging stations equipped with PV and energy storage systems [48]. To evaluate the algorithm's performance at workplace EV charging stations, various test cases were conducted using synthesized energy prices. In these scenarios, the vehicles were operated in two charging modes, and five different EVs from various manufacturers, including Tesla, Nissan, and Kia, were selected. All the information collected from [49] is provided in Table 4 where degradation cost is calculated for 80% depth of discharge.

The following three test cases have been considered in order to test the algorithm.

Table 4. Specifications of different EVs.

EV No.	EV Model	Degradation Cost (USD/kWh) [from (7)]	Power Rating (kWh)
EV1	Nissan leaf	0.85	39
EV2	Tesla Model 3	1.05	57.5
EV3	Kia e-soul	1.15	64
EV4	Tesla Model 3 long range	1.05	75
EV5	Tesla Model S plaid	1.46	95

4.2.1. Case I

In this case, all EVs will be plugged into the charger for a 12 h period (6:00 a.m. to 6:00 p.m.) with the same degradation cost. Both normal and fast charging modes were explored separately for different degradation costs. The optimal scheduling of EVs for synthesized energy price at a workplace with charging stations is depicted in Figure 8. All EVs have the same initial SoC level of 50%. Initially, all EVs consumed power to charge and, later during the peak price, injected power into the grid. In Figure 8a, it can be observed that only EV₁ has a different response profile to the rest. The reason behind this is the lowest degradation cost of EV₁. The cost would have been between –USD 2.25 and –USD 2.50 for each EV when EVs were connected without any controller. The overall savings in this mode were USD 1.78 for EV₁ and USD 1.74 for the rest of the EVs. Even though the savings seem low, the cumulative savings over the year would be significant. In Figure 8b, the responses of the EVs are shown, where all EVs were charging in fast mode. The responses from EVs were quite different from each other due to their degradation cost here as well. However, as the vehicles can charge faster, they can now utilize the peaks more effectively in this mode. The savings were USD 4.43, USD 2.96, USD 2.36, USD 2.68, and USD 3.87 for EV₁, EV₂, EV₃, EV₄, and EV₅, respectively. If no control action was taken and the EVs were kept in charging mode, then the EVs would have been charged during the peak hours. As a result, their operational costs would have been much higher.

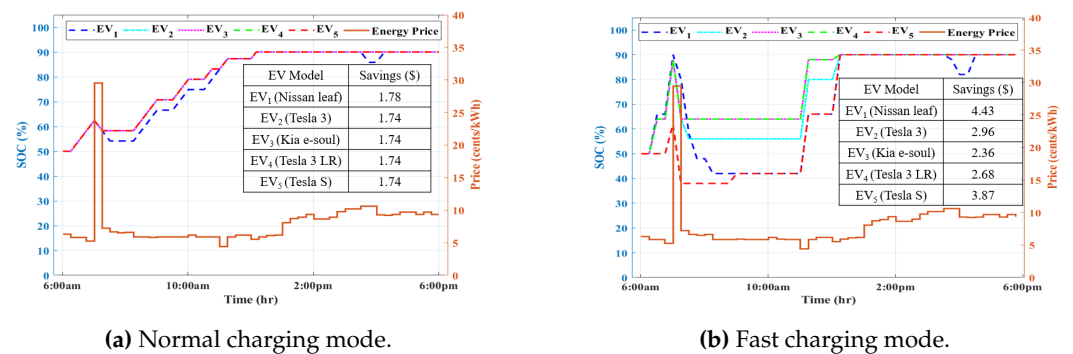


Figure 8. Response of EVs for different charging modes at a workplace with charging stations.

4.2.2. Case II

In this case, EVs had different initial SoCs, while the charging/discharging period for this case was the same as Case I. In order to fully understand the impact, only one type of EV was chosen.

In the next test case, the range of the initial SoC was set from 40% to 80% to observe the actions of the controller. The charging and discharging responses of the EVs for different initial SoCs are shown in Figure 9, where only one type of EV was used. Operational costs were higher for those EVs whose initial SoCs were lower as the vehicles needed to be charged to the desired maximum SoC level. Savings for each EV were USD 1.15, USD 1.50, USD 1.83, USD 2.16, and USD 2.49, respectively. Since vehicles with a lower initial state of charge require more energy to reach the desired SoC, their overall operational costs would be higher.

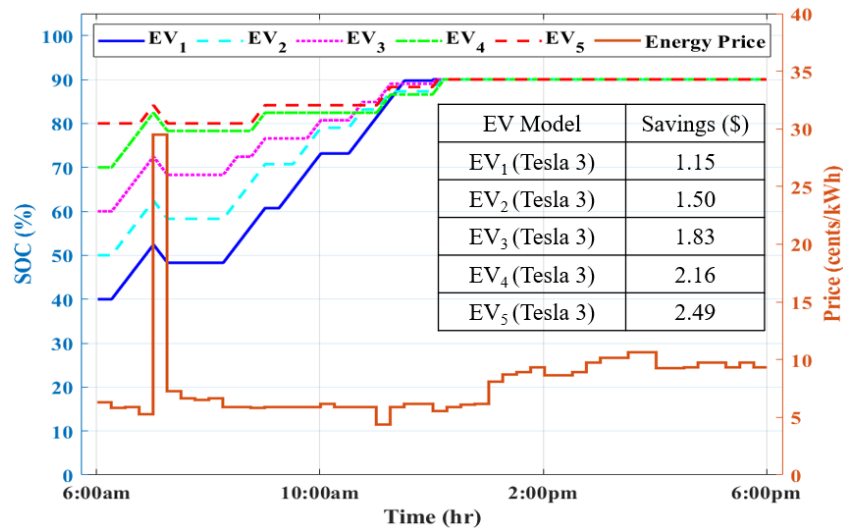


Figure 9. Output result for EVs with different initial SoCs.

4.2.3. Case III

EVs had the same initial SoC in this case. The vehicles had different charging modes, different degradation costs, and different charging speeds. The outcome for Case III is shown in Figure 10. In this case, five different EVs were connected to the charging station at the same time. However, EV₁ and EV₃ were operating in fast charging mode. Overall savings for each EV are USD 1.91, USD 1.46, USD 2.35, USD 1.05, and USD 0.97, respectively. The reason for higher savings for vehicles 1 and 3 is that they were able to use their charging speed to minimize the operation cost.

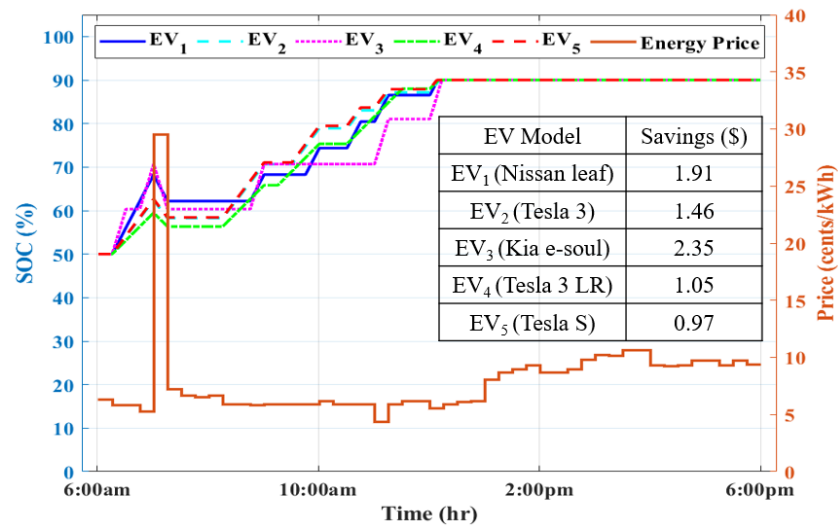
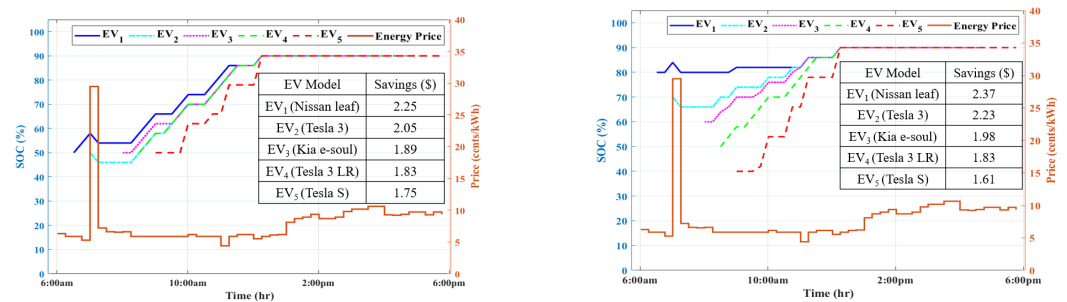


Figure 10. Output results for EVs for Case III.

4.2.4. Case IV

Vehicles can come at different hours of the day at the workplace with distinct SoCs and leave at different times in real-life scenarios. This case explored this effect on the algorithm. The assumption here is that the operational time for the workplace is between 7 a.m. and 7 p.m. So, EVs can arrive anytime between 7 a.m. and 10 a.m. for an 8 h workday. When the EVs arrive, the controller will assume it has 9 h to reach its desired SoC level unless users define different hours. As EVs can arrive with different SoCs depending on how much energy is used for the travel, this paper assumed the SoC of the EVs to be between 40% and 80% with a 10% step for simplicity.

The unpredictable nature of human behavior was analyzed in Case IV. Initially, the case study was performed by changing only the arrival time of EVs. Later, arrival/departure times and initial SoCs were randomly chosen to test the algorithm's performance. The charging/discharging period was fixed at a 9 h period, which is a typical office hour time. The output for this case can be seen in Figure 11. EV_1 and EV_2 have a lower net cost as they were able to utilize the peak price at 7:00 a.m. Moreover, these two have lower power ratings than the rest of the EVs. Figure 11a shows the responses of EVs when they had different arrival times but the same initial SoC. Figure 11b represents the responses of the EVs when both arrival and initial SoC were randomly distributed.



(a) Different arrival time.

(b) Different arrival times and initial SoCs.

Figure 11. Simulation results for Case IV.

Table 5 summarizes the savings of each EV for different test cases. The operational cost would be between –USD 3.00 and –USD 2.25 without any controller action for those EVs. So, the proposed algorithm is able to reduce operational costs for all cases.

Table 5. Savings (USD) in different test cases for workplace EVs.

Test Cases		EV1	EV2	EV3	EV4	EV5
Case I	Normal	1.78	1.74	1.74	1.74	1.74
	Fast	4.43	2.96	2.36	2.68	3.87
Case II		1.15	1.50	1.83	2.16	2.49
Case III		1.91	1.46	2.35	1.05	0.97
Case IV (a)		2.25	2.05	1.89	1.83	1.75
Case IV (b)		2.37	2.23	1.98	1.83	1.61

The current optimization framework focuses on EV SoC and operational cost minimization. However, large-scale EV charging can impact grid infrastructure, including transformer overloading and voltage stability. The simultaneous charging of multiple EVs, particularly at fast or supercharging rates, could lead to significant power demand spikes, potentially exceeding transformer capacity and causing voltage violations [50]. Additional objectives such as voltage violation cost could be added to this framework to make the problem a multi-objective problem. Then, the goal will be to find the optimal solution where both operational cost and voltage violation cost are reduced.

5. Validations Through Real-Time Simulations

The procedure for testing the algorithm for real-time setup and the comparison between the offline and real-time results are discussed in this section. Real-time validation of a controller is a necessary step that needs to be taken before any control algorithm goes to the commercial market because of the sensitive nature of the power grid. Figure 12 represents the setup for the real-time simulation used for validation purposes, where OPAL-RT [51] is used as a digital real-time simulator (DRTS). However, any other DRTS such as RTDS or Typhoon can be used as well. The DRTS transmits the current network status such as the SoC of the EV, demand, price of electricity, etc., to the Python/MAT-LAB communication interface via DNP3 over TCP/IP. The communication interface inserts the

current status of the system into the database. It also sends the system’s current status to the controller under test. Based on the received data, the controller under test optimizes and sends control decisions, i.e., reference signal, back to the DRTS via the communication interface and DNP3 over TCP/IP. The control decisions are also stored in the database by the communication layer. The database management server is necessary for storing the system’s current and historical data. The real-time simulation was performed using 50 μs. The experimental setup of the real-time simulation can be found in Figure 13 where the actual lab equipment is shown. The presented testbed comprises the following components.

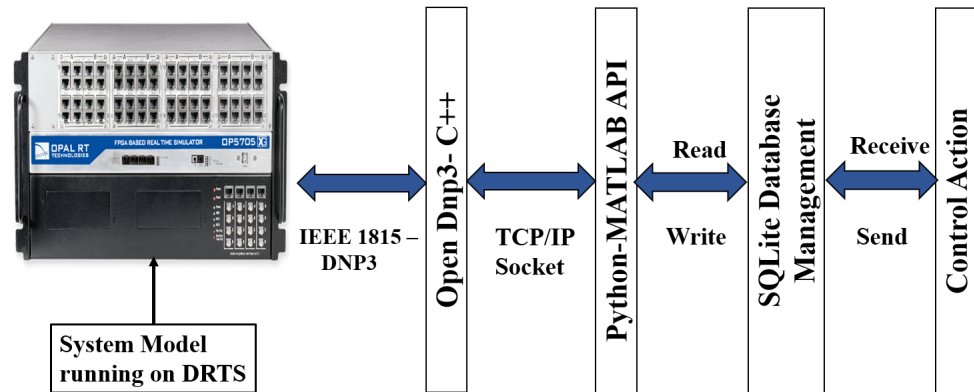


Figure 12. Digital real-time simulation setup for proposed algorithm validation.

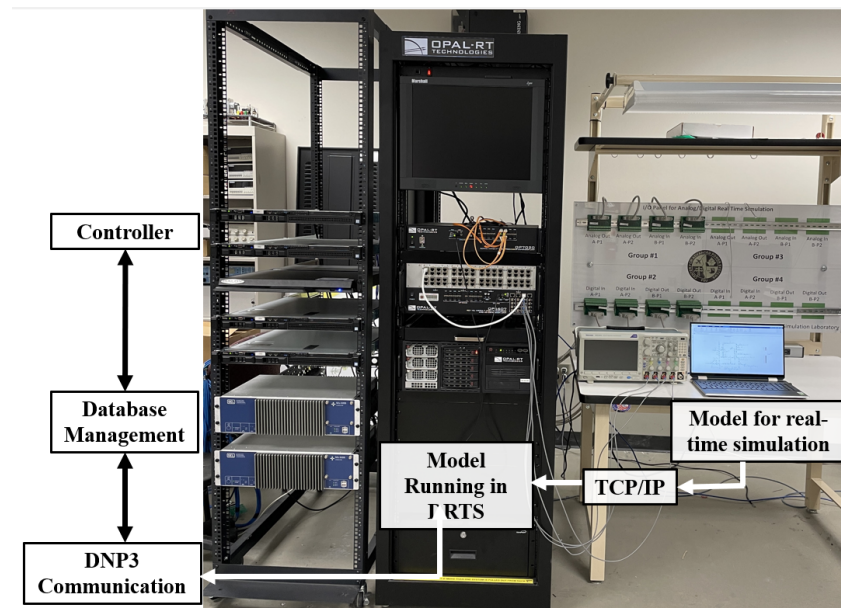


Figure 13. Experimental setup for real-time simulation.

- **Real-Time System Model:** A real-time system is made up of various models that are designed to represent and simulate the behavior and interactions of different power system components in a real environment. The transient model of the system was built in the OPAL-RT platform using RT-Lab Simulink libraries consisting of a battery of an EV from Simulink, a three-phase average model of a two-level voltage-source converter (VSC), a DC power source as a PV output, a dynamic PQ load, and a pi-section model of a three-phase transmission line. The values of PV and dynamic loads were obtained from a time series dataset with 15-minute intervals. Multiple state space nodal (SSN) solvers were used to avoid a large state space matrix that could

eventually cause overrun. These SSN blocks function as a decoupling tool, reducing a large state space matrix to smaller ones for easier and faster real-time computation.

- **Communication Interface:** The model communicated with the controller via the IEEE 1815 DNP3 communication protocol [52]. One of the main reasons for choosing this protocol is that it does not require devices to be in constant communication, thereby significantly reducing the bandwidth requirements [53].
- **Database Management Server:** SQLite [54] was used to read and write data to a database management server (DMS) deployed as an external system. This module can send data directly to outstations as well as read data from the DMS.

The test case used to validate the model involves an EV that connects to the charging station at 7:00 a.m. with an initial SoC of 60%. The vehicle departs for one hour at 11:00 a.m., returning with its SoC reduced by 10%. It then leaves the charging station again at 4:00 p.m. Figure 14 shows the real-time results compared with the offline simulation. The missing data from 11:00 a.m. to 12:00 p.m. reflects the vehicle's absence. As shown in the figure, the real-time results closely match the offline results, with a variation of around 0.5%, which is insignificant.

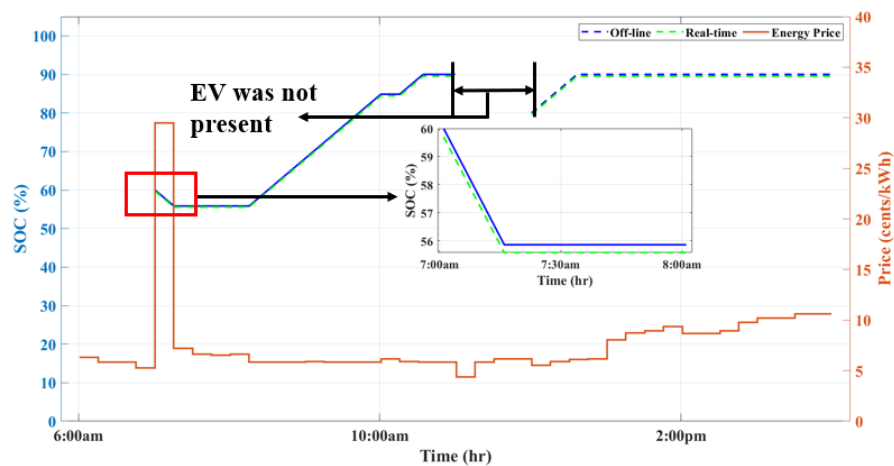


Figure 14. Comparison between real-time and offline results.

6. Conclusions

In this paper, a graph-search-based algorithm was proposed for scheduling EV charging and discharging at both the household level and workplaces with integrated PV charging stations. The method allows users to specify the total charging/discharging time and the desired SoC level of the battery. The algorithm's performance was tested under three different charging rates—normal, fast, and super—at the household level. Additionally, energy prices based on NYISO and NEISO were utilized to assess the algorithm's effectiveness. The results from various test cases indicate that the proposed algorithm significantly reduces the cost of EV operation across different modes. When compared to PSO and GA, the algorithm outperforms them by approximately 5% and 4%, respectively. For workplace testing, five different electric vehicles were used in various uncertain conditions, demonstrating that the proposed method can reduce the operational costs of all workplace EVs compared to those without a controller. An experimental test system, modeled on a digital real-time simulator with PV, loads, and EVs, and using the DNP3 communication protocol, confirmed that offline and real-time results were nearly identical, validating the efficacy of the proposed model. The algorithm is able to minimize operational costs for EV users while simultaneously reducing peak demand encourages demand-side management (DSM) and energy efficiency. By shifting EV charging to off-peak hours and enabling V2G capabilities during peak demand, this approach could contribute to lower electricity prices, reduce strain on grid infrastructure, and increase grid flexibility.

The proposed model is evaluated for small-scale EVs. As the number of EVs increases, the solution space for the scheduling problem grows exponentially due to the combinatorial nature of the optimization process. The evaluation of multiple nodes and edges in the solution space, particularly in a real-time scenario, may become computationally expensive. Charging and discharging schedules of EVs are often independent, and the graph-search process can be parallelized, with multiple processors working on different EVs simultaneously. This would significantly reduce the time required for finding optimal solutions in large-scale systems. In the future, we plan to incorporate dynamic pricing, more non-linear behaviors from the EVs, and a distributed approach where local controllers will handle smaller groups of EVs, reducing the burden on a central controller.

Author Contributions: Conceptualization, M.J.A.S. and S.O.; methodology, M.J.A.S.; software, M.J.A.S. and M.M.I.; validation, M.J.A.S., M.M.I. and S.O.; formal analysis, M.J.A.S.; investigation, M.J.A.S.; resources, M.J.A.S. and M.O.F.; data curation, M.J.A.S.; writing—original draft preparation, M.J.A.S.; writing—review and editing, M.J.A.S., M.M.I., S.O. and M.O.F.; visualization, M.J.A.S.; supervision, M.O.F.; project administration, M.O.F.; funding acquisition, M.O.F. All authors have read and agreed to the published version of the manuscript.

Funding: This research was funded by the Department of Electrical and Computer Engineering, FAMU-FSU College of Engineering, Florida State University.

Data Availability Statement: Data used for generating the reported results can be found at [36,39,40,49]: Tesla (<http://www.tesla.com>), ISO New England (<http://www.iso-ne.com>), New York ISO (<https://www.nyiso.com>), Electric Vehicle Database (<http://ev-database.org>.)

Acknowledgments: ChatGPT-4's AI tool was used to check and fix a few grammatical and spelling errors in the article.

Conflicts of Interest: The authors declare no conflicts of interest.

Abbreviations

The following abbreviations are used in this manuscript:

DER	Distributed energy resource
DMS	Database management server
DNP3	Distributed Network Protocol
DRTS	Digital real-time simulator
EV	Electric vehicle
GA	Genetic algorithm
ISO	Independent system operator
NEISO	New England Independent System Operator
NYISO	New York Independent System Operator
PSO	Particle swarm optimization
PV	Photovoltaic
RTP	Real-time price
SSN	State space nodal
SoC	State of charge
V2G	Vehicle-to-grid
VSC	Voltage source converter

References

1. Dutta, A.; Ganguly, S.; Kumar, C. Coordinated control scheme for EV charging and volt/var devices scheduling to regulate voltages of active distribution networks. *Sustain. Energy Grids Netw.* **2022**, *31*, 100761. [[CrossRef](#)]
2. Srinivasan, D.; Rajgarhia, S.; Radhakrishnan, B.M.; Sharma, A.; Khincha, H.P. Game-Theory based dynamic pricing strategies for demand side management in smart grids. *Energy* **2017**, *26*, 132–143. [[CrossRef](#)]
3. Tomašov, M.; Straka, M.; Martinko, D.; Bracinič, P.; Buzna, L. A Feasibility Study of Profiting from System Imbalance Using Residential Electric Vehicle Charging Infrastructure. *Energies* **2023**, *16*, 7820. [[CrossRef](#)]
4. Khwanrit, R.; Javaid, S.; Lim, Y.; Charoenlarnpopparut, C.; Tan, Y. Optimal Vehicle-to-Grid Strategies for Energy Sharing Management Using Electric School Buses. *Energies* **2024**, *17*, 4182. [[CrossRef](#)]

5. Yan, Q.; Gao, Y.; Xing, L.; Xu, B.; Li, Y.; Chen, W. Optimal Scheduling for Increased Satisfaction of both Electric Vehicle Users and Grid Fast-Charging Stations by SOR& KANO and MVO in PV-Connected Distribution Network. *Energies* **2024**, *17*, 3413. [[CrossRef](#)]
6. Chen, Q.; Folly, K.A. Application of Artificial Intelligence for EV Charging and Discharging Scheduling and Dynamic Pricing: A Review. *Energies* **2023**, *16*, 146. [[CrossRef](#)]
7. Erdogan, G.; Fekih, Hassen, W. Charging Scheduling of Hybrid Energy Storage Systems for EV Charging Stations. *Energies* **2023**, *16*, 6656. [[CrossRef](#)]
8. Jin, H.; Lee, S.; Nengroo, S.H.; Har, D. Development of Charging/Discharging Scheduling Algorithm for Economical and Energy-Efficient Operation of Multi-EV Charging Station. *Appl. Sci.* **2022**, *12*, 4786. [[CrossRef](#)]
9. El Harouri, K.; El Hani, S.; Naseri, N.; Elbouchikhi, E.; Benbouzid, M.; Skander-Mustapha, S. Hybrid Control and Energy Management of a Residential System Integrating Vehicle-to-Home Technology. *Designs* **2023**, *7*, 52. [[CrossRef](#)]
10. Al-Ogaili, A.S.; Hashim, T.J.T.; Rahmat, N.A.; Ramasamy, A.K.; Marsadek, M.B.; Faisal, M.; Hannan, M.A. Review on scheduling, clustering, and forecasting strategies for controlling electric vehicle charging: Challenges and recommendations. *IEEE Access* **2019**, *7*, 128353–128371. [[CrossRef](#)]
11. Guo, Y.; Xiong, J.; Xu, S.; Su, W. Two-stage economic operation of microgrid-like electric vehicle parking deck. *IEEE Trans. Smart Grid* **2015**, *7*, 1703–1712. [[CrossRef](#)]
12. Wu, D.; Zeng, H.; Lu, C.; Boulet, B. Two-stage energy management for office buildings with workplace EV charging and renewable energy. *IEEE Trans. Transp. Electrification* **2017**, *3*, 225–237. [[CrossRef](#)]
13. Nazari-Heris, M.; Mirzaei, M.A.; Asadi, S.; Mohammadi-Ivatloo, B.; Zare, K.; Jebelli, H. A hybrid robust-stochastic optimization framework for optimal energy management of electric vehicles parking lots. *Sustain. Energy Technol. Assessments* **2021**, *47*, 101467. [[CrossRef](#)]
14. Aljohani, T. M. Multilayer Iterative Stochastic Dynamic Programming for Optimal Energy Management of Residential Loads with Electric Vehicles. *Int. J. Energy Res.* **2024**, *1*, 6842580. [[CrossRef](#)]
15. Shao, S.; Harirchi, F.; Dave, D.; Gupta, A. Preemptive scheduling of EV charging for providing demand response services. *Sustain. Energy, Grids Netw.* **2023**, *33*, 100986. [[CrossRef](#)]
16. Long, T.; Jia, Q.S.; Wang, G.; Yang, Y. Efficient real-time EV charging scheduling via ordinal optimization. *IEEE Trans. Smart Grid* **2021**, *12*, 4029–4038. [[CrossRef](#)]
17. Yang, Y.; Jia, Q.S.; Deconinck, G.; Guan, X.; Qiu, Z.; Hu, Z. Distributed coordination of EV charging with renewable energy in a microgrid of buildings. *IEEE Trans. Smart Grid* **2017**, *9*, 6253–6264. [[CrossRef](#)]
18. Qian, K.; Adam, R.; Brehm, R. Reinforcement learning based EV charging scheduling: A novel action space representation. In Proceedings of the 2021 IEEE PES Innovative Smart Grid Technologies-Asia (ISGT Asia), Brisbane, Australia, 5–8 December 2021; IEEE: Piscataway, NJ, USA, 2021; pp. 1–5.
19. Yan, L.; Chen, X.; Zhou, J.; Chen, Y.; Wen, J. Deep reinforcement learning for continuous electric vehicles charging control with dynamic user behaviors. *IEEE Trans. Smart Grid* **2021**, *12*, 5124–5134. [[CrossRef](#)]
20. Li, H.; Wan, Z.; He, H. Constrained EV charging scheduling based on safe deep reinforcement learning. *IEEE Trans. Smart Grid* **2019**, *11*, 2427–2439. [[CrossRef](#)]
21. Newaz, A.; Ospina, J.; Faruque, M.O. Controller hardware-in-the-loop validation of a graph search based energy management strategy for grid-connected distributed energy resources. *IEEE Trans. Energy Convers.* **2019**, *35*, 520–528. [[CrossRef](#)]
22. Ketabi, A.; Karimizadeh, A.; Shahidepour, M. Optimal generation units start-up sequence during restoration of power system considering network reliability using bi-level optimization. *Int. J. Electr. Power Energy Syst.* **2019**, *104*, 772–783. [[CrossRef](#)]
23. Owais, S.; Shohan, M.J.A.; Islam, M.M.; Faruque, M.O. Management of grid connected energy storage systems employing real-time energy price. *J. Energy Storage* **2024**, *92*, 112097. [[CrossRef](#)]
24. Chen, T.; Zhang, X.P.; Wang, J.; Li, J.; Wu, C.; Hu, M.; Bian, H. A review on electric vehicle charging infrastructure development in the UK. *J. Mod. Power Syst. Clean Energy* **2020**, *8*, 193–205. [[CrossRef](#)]
25. Cheikh-Mohamad, S.; Sechilariu, M.; Locment, F.; Krim, Y. Pv-powered electric vehicle charging stations: Preliminary requirements and feasibility conditions. *Appl. Sci.* **2021**, *11*, 1770. [[CrossRef](#)]
26. Saw, L.H.; Somasundaram, K.; Ye, Y.; Tay, A.A.O. Electro-thermal analysis of Lithium Iron Phosphate battery for electric vehicles. *J. Power Sources* **2014**, *249*, 231–238. [[CrossRef](#)]
27. Alhanouti, M.; Gießler, M.; Blank, T.; Gauterin, F. New Electro-Thermal Battery Pack Model of an Electric Vehicle. *Energies* **2016**, *9*, 563. [[CrossRef](#)]
28. Jörg, I. *Physically Based Impedance Modelling of Lithium-Ion Cells*; KIT Scientific Publishing: Karlsruhe, Germany, 2014; Volume 27.
29. Tremblay, O.; Dessaint, L.A. Experimental validation of a battery dynamic model for EV applications. *World Electr. Veh. J.* **2009**, *3*, 289–298. [[CrossRef](#)]
30. Zhu, C.; Li, X.; Song, L.; Xiang, L. Development of a theoretically based thermal model for lithium ion battery pack. *J. Power Sources* **2013**, *223*, 155–164. [[CrossRef](#)]
31. Eom, J.K.; Lee, S.R.; Ha, E.J.; Choi, B.Y.; Won, C.Y. Economic dispatch algorithm considering battery degradation characteristic of energy storage system with PV system. In Proceedings of the 2014 17th International Conference on Electrical Machines and Systems (ICEMS), Hangzhou, China, 22–25 October 2014; pp. 849–854.

32. Duchoň, F.; Babinec, A.; Kajan, M.; Beňo, P.; Florek, M.; Fico, T.; Jurišica, L. Path planning with modified a star algorithm for a mobile robot. *Procedia Eng.* **2014**, *96*, 59–69. [CrossRef]
33. Shohan, M.J.A.; Faruque, M.O.; Foo, S.Y. Forecasting of electric load using a hybrid LSTM-neural prophet model. *Energies* **2022**, *15*, 2158. [CrossRef]
34. Pang, Z.; Niu, F.; O'Neill, Z. Solar radiation prediction using recurrent neural network and artificial neural network: A case study with comparisons. *Renew. Energy* **2020**, *156*, 279–289. [CrossRef]
35. Shuvo, S.S.; Islam, M.M. LSTM Based Load Prediction for Distribution Power Grid with Home EV Charging. In Proceedings of the 2022 IEEE Kansas Power And Energy Conference (KPEC), Manhattan, KS, USA, 25–26 April 2022; pp. 1–5.
36. Tesla Model 3. Available online: <http://www.tesla.com> (accessed one 23 September 2023).
37. Witt J. Depth of Discharge Basics for Every EV Owner. Available online: <http://www.recurrentauto.com/research/depth-of-discharge-ev> (accessed on 23 September 2023).
38. Meeker, R.; Steurer, M.; Faruque, M.D.; Langston, J.; Schoder, K.; Ravindra, H.; Reedy, B. *High Penetration Solar pv Deployment Sunshine State Solar Grid Initiative (Sungrin) (No. DOE-FSU-04682-1)*; Florida State University: Tallahassee, FL, USA, 2015.
39. ISO New England. Available online: <http://www.iso-ne.com> (accessed on 13 September 2023).
40. NewYork ISO. Available online: <https://www.nyiso.com> (accessed on 23 September 2023).
41. Pang, Z.; Chen, Y.; Zhang, J.; O'Neill, Z.; Cheng, H.; Dong, B. How much HVAC energy could be saved from the occupant-centric smart home thermostat: A nationwide simulation study. *Appl. Energy* **2021**, *283*, 116251. [CrossRef]
42. Yin, W.J.; Ming, Z.F. Electric vehicle charging and discharging scheduling strategy based on local search and competitive learning particle swarm optimization algorithm. *J. Energy Storage* **2021**, *42*, 102966. [CrossRef]
43. Shuvo, S.S.; Islam, M.M. Optimal Dispatch for A Microgrid with Distributed Generations and EV Charging Load. In Proceedings of the 2023 IEEE Power & Energy Society Innovative Smart Grid Technologies Conference (ISGT), Washington, DC, USA, 16–19 January 2023; pp. 1–5.
44. Marini, F.; Walczak, B. Particle swarm optimization (PSO). A tutorial. *Chemom. Intell. Lab. Syst.* **2015**, *149*, 153–165. [CrossRef]
45. Whitley, D. A genetic algorithm tutorial. *Stat. Comput.* **1994**, *4*, 65–85. [CrossRef]
46. Elmehdi, M.; Abdelilah, M. Genetic algorithm for optimal charge scheduling of electric vehicle fleet. In Proceedings of the 2nd International Conference on Networking, Information Systems & Security, Rabat, Morocco, 27–29 March 2019; pp. 1–7.
47. Erdogan, N.; Pamucar, D.; Kucuksari, S.; Devenci, M. A hybrid power Heronian function-based multicriteria decision-making model for workplace charging scheduling algorithms. *IEEE Trans. Transp. Electrification* **2022**, *9*, 1564–1578. [CrossRef]
48. Amry, Y.; Elbouchikhi, E.; Le Gall, F.; Ghogho, M.; El Hani, S. Optimal sizing and energy management strategy for EV workplace charging station considering PV and flywheel energy storage system. *J. Energy Storage* **2022**, *62*, 106937. [CrossRef]
49. Electric Vehicle Database. Available online: <http://ev-database.org> (accessed on 21 March 2023).
50. Khalid, M.; Thakur, J.; Bhagavathy, S.M.; Topel, M. Impact of public and residential smart EV charging on distribution power grid equipped with storage. *Sustain. Cities Soc.* **2024**, *104*, 105272. [CrossRef]
51. OPAL-RT Technologies. Available online: <http://www.opal-rt.com> (accessed on 23 December 2023).
52. Soliman, A.S.; Saad, A.A.; Mohammed, O. Securing networked microgrids operation through DNP3 protocol implementation. In Proceedings of the 2021 IEEE Industry Applications Society Annual Meeting (IAS), Vancouver, BC, Canada, 10–14 October 2021; pp. 1–6.
53. IEEE Standards Association. *IEEE Standard for Electric Power Systems Communications-Distributed Network Protocol (dnp3)*; IEEE: Piscataway, NJ, USA, 2014.
54. SQLite Home. Available online: <http://www.sqlite.org/index.html> (accessed on 20 December 2023).

Disclaimer/Publisher's Note: The statements, opinions and data contained in all publications are solely those of the individual author(s) and contributor(s) and not of MDPI and/or the editor(s). MDPI and/or the editor(s) disclaim responsibility for any injury to people or property resulting from any ideas, methods, instructions or products referred to in the content.